Polymersomes with a smectic liquid crystal structure and AIE fluorescence

Nian Zhang, Yujiao Fan, Hui Chen, Sylvain Trépout, Annie Brûlet, Min-Hui Li

Polymersomes with smectic liquid crystal structure and AIE fluorescence

Nian Zhang, [a,†] Yujiao Fan, [a,†] Hui Chen,[a,b] Sylvain Trépout,[c] Annie Brûlet,[d] and Min-Hui Li*[a]

Received 22nd December 2021,
Accepted 17th January 2022

DOI: 10.1039/d1py01686e

A series of amphiphilic diblock copolymers PEG-TPE-*b*-PAChol containing a cholesterol-based smectic liquid crystal block PAChol and a tetraphenylethene AIEgen situated between hydrophilic PEG and hydrophobic PAChol blocks were prepared by RAFT polymerization. The liquid crystal properties of the block copolymers were first characterized. One of the copolymers, PEG_{45}-TPE-*b*-$PAChol_{16}$, with a hydrophilic weight ratio of 18% was chosen for the self-assembly study using the nanoprecipitation method in dioxane/water and THF/water systems. The co-solvent (THF or dioxane) had significant effect on its self-assembly behaviors. The characterization by cryo-EM showed that elongated ellipsoidal or tubular polymersomes with smectic ordering in the membrane were formed in the dioxane/water system. In contrast, spherical solid nanoparticles were obtained in THF/water system as observed by SEM. All polymersomes and nanoparticles showed AIE fluorescence. The present work shows the possibility to obtain elongated polymersomes with both smectic LC orders and AIE fluorescence. By replacing the prototypical TPE with AIEgens that can be excited in longer wavelength than UV, these cholesterol-based polymersomes and nanoparticles can be designed as fluorescent carriers of drugs for possible theranostic applications.

Introduction

Liquid crystal (LC) polymersomes are a special type of polymer vesicles with thermotropic LC phases displayed in the lyotropic polymer-based bilayer membrane.[1] LC polymersomes exhibit either interesting non-spherical morphology because of the LC phase like smectic one,[2] or stimuli-responsive features due to the sensitivity of chain conformation to external stimuli such as light.[3] LC polymersomes are usually prepared by the self-assembly of amphiphilic block copolymers where the hydrophobic block is a thermotropic nematic or smectic LC polymer. Our group and others have reported several LC polymersomes based on side-chain LC polymers.[4-12] The self-assembly of amphiphilic LC block copolymers is affected not only by the relative sizes of two constituting blocks, but also by the LC order and the chain conformation in the LC block, which results in more complicated self-assembly behaviours than those of classical coil-coil block copolymers.[2] Spherical,[4, 5] ellipsoidal[7] and faceted[6] LC polymersomes have been reported, which disclosed the important relationship between the orientational and positional LC order and the curved geometry of a two-dimensional membrane.[2] Among them, polymersomes made from poly(ethylene glycol)-*block*-poly(cholesteryl-based acrylate) (PEG-*b*-PAChol)[7] shown in Figure 1a is of special interest for the following reasons. Firstly, the cholesterol is a biosourced and biocompatible LC moiety; it has been exploited as building block of polymer micelles for the delivery of with anticancer drugs due to its favourable hydrophobic interaction with drugs.[13] Secondly, PAChol exhibits a smectic LC phase extending up to at least 100°C and a glass transition higher than room temperature (precise values depending on the molecular weight).[7] Thirdly, PEG-*b*-PAChol forms ellipsoidal or elongated polymersomes in water, where the smectic phase or glassy smectic phase play the role of physical cross-linking and ensure the stability and robustness.[7, 9] The elongated vesicular shape may be an advantage when they are used as carriers of imaging agents or drugs, because it has been shown that the elongated shape of the carrier does affect the pharmacokinetics and *in vivo* distribution,[14] for example, by persisting longer after intravenous injection and possessing higher drug loading than their spherical counterparts.[15, 16] Therefore, it is interesting to investigate this cholesterol-based LC polymersome for the bioimaging and controlled release. In our previous work, a disulfide bridge (-S–S-) was introduced between the hydrophilic PEG block and the hydrophobic PAChol block (Figure 1b) to get the reduction-responsive LC polymer PEG-SS-*b*-PAChol. A robust reduction-responsive polymersome based on PEG-SS-*b*-PAChol was achieved, which has been used to encapsulate the calcein as a model molecule. The release of the calcein from the polymersome was triggered by glutathione (GSH) both in PBS suspension and *in vitro* inside the macrophage cells with artificially enhanced GSH concentration (≥35 mM).[17] Moreover, cell viability tests have shown that nanoparticles formed by both cholesterol-based polymers (PEG-SS-*b*-PAChol and PEG-*b*-PAChol) were not cytotoxic.[17] In this work, we want to explore

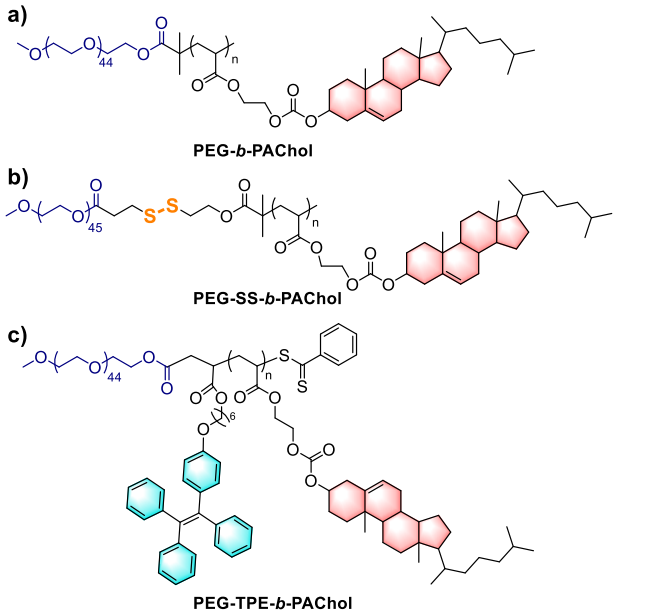

Figure 1. Amphiphilic block copolymers with cholesteryl-based LC polymer, PEG-*b*-PAChol,[7] PEG-SS-PAChol,[17] and PEG-TPE-*b*-PAChol.

the cholesterol-based LC polymersome as imaging nanoparticle by introducing a fluorescent moiety (tetraphenylethene, TPE) between PEG and PAChol blocks (PEG-TPE-*b*-PAChol in Figure 1c).

Fluorescent materials, in particular organic dyes, have been widely used as bioimaging agents. When organic dyes are integrated into polymer-based nanostructures,[18-20] the optical signals could be amplified due to the incorporation of several fluorophore molecules in the same nanoparticle. In addition, the polymer structures, in some cases, contribute to the uniform distribution of the involved fluorophores, which could avoid aggregation-caused quenching (ACQ) or photo-bleaching to a certain extent. More excitedly, luminogens with aggregation-induced emission (AIE) characteristics, that circumvents the ubiquitous ACQ phenomenon, have been largely developed recently as efficient fluorescent visualizers for organelles imaging and drug delivery monitoring.[21-28] The combination of polymer nanostructures with AIE luminogens (AIEgens) provide then innovative approaches to cell/tissue imaging and to *in vivo* study of drug bio-distribution.[27, 28] For this purpose, several systems of polymersomes with AIE properties have been published.[29-39] In this work, we introduce a typical AIEgen, tetraphenylethylene (TPE) in the polymer structure as shown in Figure 1c. The TPE group has been inserted between the hydrophilic block PEG and the hydrophobic block PAChol, in order to preserve the smectic organisation of the hydrophobic block. A series of block copolymers PEG_{45}-TPE-*b*-$PAChol_n$ with different hydrophilic ratios (f_{PEG} = 8 - 24 wt%) were synthesized and characterized. One of them, PEG_{45}-TPE-*b*-$PAChol_{16}$ (f_{PEG} = 18 wt%) was taken as an example to study the self-assembly by nanoprecipitation in dioxane/water and THF/water systems. Elongated smectic polymersomes were obtained in dioxane/water system, while spherical nanoparticles were obtained in THF/water system. Both polymersomes and spherical nanoparticles exhibited AIE fluorescence under UV light.

Experimental

Materials

Bromobenzene (C_6H_5Br, 99%, Acros), magnesium (Mg, >99%, Sigma-Aldrich), Iodine (I_2, 99.5%, Alfa Aesar), carbon disulfide (CS_2, Fisher Scientific), hydrochloric acid (HCl, 37%, VWR), maleic anhydride ($C_4H_2O_3$, 98%, Alfa Aesar), carbon tetrachloride (CCl_4, Sigma-Aldrich), N, N'-dicyclohexylcarbodiimide ($C_{13}H_{22}N_2$, DCC, Fluka), 4-dimethylaminopyridine ($C_7H_{10}N_2$, DMAP, Sigma-Aldrich), 2-Hydroxyethyl acrylate (97%, Alfa Aesar), cholesteryl chloroformate (95%, Sigma-Aldrich) and pyridine (99.8%, Sigma-Aldrich) were used as received. 2,2'-azobis(isobutyronitrile) (AIBN, Sigma-Aldrich) was recrystallized from ethanol for three times before use. Poly (ethylene glycol) monomethyl ether ($mPEG_{45}$-OH, M_n = 2000 Da, Fluka) was purified by precipitation in diethyl ether for three times before use. Dry dichloromethane and THF was taken from the solvent purification system (SPS). 1,4-dioxane used for polymerization was dried by refluxing with calcium hydride. The monomer AChol (cholesteryl acryloyloxy ethyl carbonate) was synthesized by a one-step reaction between 2-hydroxyethyl acrylate and cholesteryl chloroformate as detailed in Supporting Information (SI, Figure S1).

Methods

Synthesis of amphiphilic LC diblock copolymer PEG-TPE-*b*-PAChol. The diblock copolymer PEG-TPE-*b*-PAChol was synthesized by RAFT polymerization using TPE-functionalized macro chain transfer agent (CTA), mPEG-TPE-CTA, as shown in Figure 2a. For mPEG-TPE-CTA preparation, benzodithioic acid and 6-hydroxyhexyloxy-substituted TPE (TPE-OH) were firstly synthesized as described previously.[40, 41] TPE-OH was further transformed into a TPE derivative bearing an alkene group and a carboxylic acid group (TPE-CH=CH-COOH) by reacting with maleic anhydride. Then TPE-CH=CH-COOH was reacted with benzodithioic acid by thiol-ene coupling reaction to obtain a new TPE derivative bearing a benzodithioate group and carboxylic acid group. Finally, the esterification of this functional TPE derivative by $mPEG_{45}$-OH in the presence of DCC and DMAP was performed to get $mPEG_{45}$-TPE-CTA. The product was purified by column chromatography with methanol and dichloromethane mixture (volume ratio 1:30) as the eluents to remove unreacted $mPEG_{45}$-OH. The obtained product was characterized by ^{1}H NMR and SEC, as shown in Figure S3-4. The M_n of the prepared mPEG-TPE-CTA was 2680 Da as calculated by ^{1}H NMR and its polydispersity index (M_w/M_n) was about 1.09 evaluated by SEC results.

Taking the synthesis of PEG_{45}-TPE-*b*-$PAChol_{16}$ as an example, the typical RAFT polymerization process was as follows: AChol (226 mg, 0.429 mmol), mPEG-TPE-CTA (103 mg, 0.0429 mmol) and AIBN (1.41 mg, 0.0086 mmol) were added into a 15 mL Schlenk tube equipped with a Teflon coated stirring bar. Then 1.5 mL dry 1,4-dioxane was added. After the solution became clear, the Schlenk tube was degassed by three freeze-pump-thaw cycles and then immersed into an oil bath of 80 °C. The mixture was stirred at 80 °C for 24 h, after which the polymerization was terminated by freezing the mixture in liquid nitrogen. The mixture was then added drop-by-drop into cold methanol to precipitate the crude PEG-TPE-*b*-PAChol diblock copolymer, which was further purified twice using dichloromethane/methanol as solvent/precipitant pair. The dried pure polymer was obtained as a pink solid (220 mg, yield: 67%). The synthesis of other PEG-TPE-*b*-PAChol with different PAChol block lengths was similar except that the different

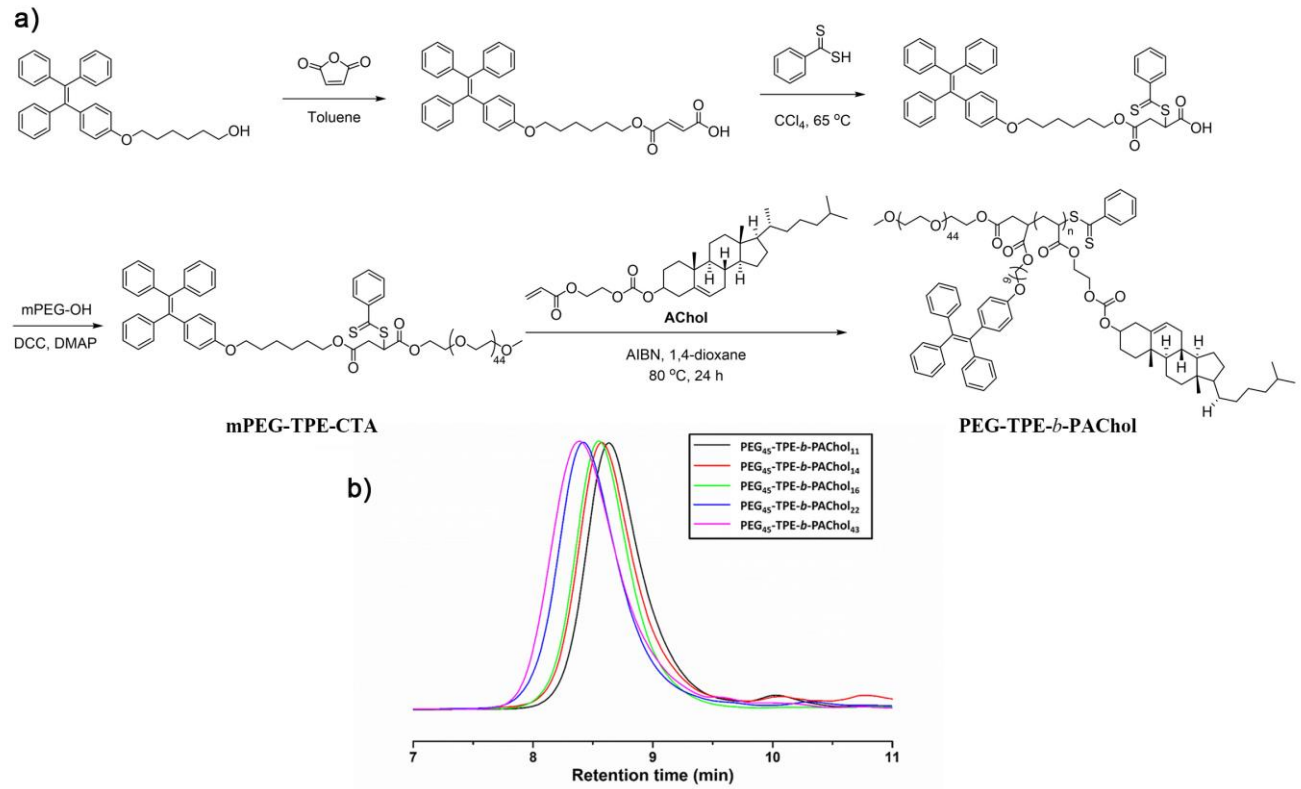

Figure 2. (a) Synthetic route to the TPE-functionalized macro chain transfer agent mPEG-TPE-CTA and the LC amphiphilic block copolymer PEG-TPE-*b*-PAChol. (b) SEC chromatogram of PEG-TPE-*b*-PAChol copolymers (Table 1) with THF as the eluent.

amounts of AChol, mPEG-TPE-CTA and 1,4-dioxane were used on keeping the concentration of mPEG-TPE-CTA at 0.028 M. The details are given in Table S1. The molecular weights and molecular weight distributions characterized by ^{1}H NMR and SEC of all copolymers are listed in Table 1.

Liquid crystalline properties of diblock copolymer PEG-TPE-*b*-PAChol. The mesomorphic properties of block copolymers in pure stat were studied by thermal polarizing optical microscopy (POM), differential scanning calorimetry (DSC), and small angle X-ray scattering (SAXS) (see SI for instrumental details). The SAXS sample is a fiber drawn by hand with a pair of tweezers from a molten copolymer at a temperature just below the isotropic-liquid crystal phase.

Self-assembly of PEG_{45}-TPE-*b*-$PAChol_{16}$. The self-assembly was performed using a classical nanoprecipitation method. Typically, the copolymer was firstly dissolved in THF or dioxane, which was a good solvent for both PEG and PAChol blocks. The initial concentration of the copolymer in organic solvent was 2 mg/mL. Then deionized water was added slowly to the THF or dioxane solution (around 3 uL/min) with gently shaking until the water content reached 75 wt%. THF or dioxane was removed by dialysis against deionized water for 3 days in a 3500 Da cut off cellulose dialysis bag. Finally, the aqueous solution of the PEG_{45}-TPE-*b*-$PAChol_{16}$ self-assemblies with a concentration of about 0.5 mg/mL (polymer concentration) was obtained.

Studies of AIE properties. The fluorescence quantum yield of the AIE polymersomers or nanoparticles in aqueous solution were obtained by comparing the integrated fluorescence spectra of the self-assembly solution with the fluorescence spectrum of a standard fluorogen, 9,10-diphenylanthracene, in ethanol (excitation wavelength: 355 nm) as described in the literature (see SI for detail).[42]

For the detection of AIE phenomena in organic solvent/water mixtures with different water fractions, a classical process was used. Typically, 25.6mg copolymer was dissolved in 1mL THF (or dioxane), and an aliquote of 131 μL of the copolymer solution was added into each of the 7 glass vials. Then the mixture of water and THF (or dioxane) with different volume fraction of water (f_w = 0%, 20%, 40%, 60%, 80%, 90% and 99%) was added, respectively, into each of the glass vials containing the tinny polymer solution to reach the copolymer concentration of 10^{-4} mol/L (3.36 mg/mL). All mixtures in vials were shaken overnight.

Results and Discussion

1. Synthesis of amphiphilic LC diblock copolymer PEG-TPE-*b*-PAChol

Five LC amphiphilic diblock copolymers PEG_{45}-TPE-*b*-$PAChol_n$ with different PAChol block lengths and hydrophilic ratios (Table 1) were prepared according to processes shown in Figure 2a (see Methods and Figure S1-4 for details).

The TPE-functionalized macro chain transfer agent (CTA), mPEG-TPE-CTA, was first synthesized from monomethoxy polyethylene glycol ($mPEG_{45}$-OH, 2000 Da). The diblock copolymer PEG-TPE-*b*-PAChol was then synthesized by RAFT

Table 1. LC amphiphilic block copolymers PEG-TPE-*b*-PAChol.

Sample	DP_{PAChol} [a]	M_n [b]	$Đ$ [c]	f_{PEG} [d] (wt%)
PEG_{45}-TPE-*b*-$PAChol_{11}$	11	8500	1.17	24%
PEG_{45}-TPE-*b*-$PAChol_{14}$	14	10100	1.18	20%
PEG_{45}-TPE-*b*-$PAChol_{16}$	16	11200	1.19	18%
PEG_{45}-TPE-*b*-$PAChol_{22}$	22	14300	1.23	14%
PEG_{45}-TPE-*b*-$PAChol_{43}$	43	25400	1.24	8%

[a] Number average degrees of polymerization (DP_{PAChol}) and molecular weights ($M_{n,\ PAChol}$) of PAChol block evaluated by ^{1}H NMR.

[b] Number average molecular weights of block copolymers evaluated by ^{1}H NMR. M_n = $M_{n,\ PAChol}$ + 2680 (Da) (2680 Da being the molecular weight of mPEG-TPE-CTA).

[c] Polydispersity index ($Đ = M_w/M_n$) of copolymers calculated from weight and number average molecular weight (M_w and M_n) evaluated by size exclusion chromatography (SEC) with tetrahydrofuran as eluent and polystyrene as standard.

[d] Weight ratio of the hydrophilic part (f_{PEG}) calculated by the molecular weight of PEG (2000 Da) over M_n of PEG-TPE-*b*-PAChol.

polymerization using different feeding ratios of monomer/CTA (AChol/mPEG-TPE-CTA), as shown in Table S1. The chemical structures of the copolymers were confirmed by ^{1}H NMR (Figure S5). The degree of polymerization (DP) and M_n of PAChol was calculated by comparing the integrated areas of the proton peak from the cholesteryl groups (I_g of peak g) and that from the methyl group at the end of PEG chain (I_a of peak a) in the ^{1}H NMR spectrum (see Figure S5), *i.e.*, $DP_{PAChol} = 3*(I_g/I_a)$. The SEC chromatograms of the five copolymers (Figure 2b) show unimodal peaks with narrow distributions ($Đ$ = 1.17–1.24). So, these amphiphilic LC block copolymers are suitable for the study of their self-assembly behaviours and AIE properties.

2. Liquid crystal properties of amphiphilic LC diblock copolymer PEG-TPE-*b*-PAChol

Recall that the homopolymer $PAChol_{10}$ is a smectic polymer with the phase sequence: g – 68°C - SmA_d - 156°C - I, where the interdigitated smectic A phase (SmA_d) has a smectic layer spacing of P = 4.29 nm, which corresponds to a value between l and 2l, l = 2.61 nm being the wholly extended length of the Chol mesogen estimated by Dreiding models.[7] Here, three copolymer samples PEG_{45}-TPE-*b*-$PAChol_n$ (n = 11, 14, 16) were studied by DSC, POM and X-ray scattering to elucidate their liquid crystal phases in pure state. Take PEG_{45}-TPE-*b*-$PAChol_{16}$ as an example for DSC study (scanning rate ±10°C/min, see Figure S6 and Table S2 in SI). Upon first heating the pristine sample obtained from purification by precipitation, a melting point (T_m) of PEG at 45.7°C, a glass transition T_g of $PAChol_{16}$ at 66.9°C and several crystals melting points of $PAChol_{16}$ around 143°C and 152°C were observed until isotropic phase. On cooling from 160°C, the transition from isotropic to smectic (SmA_d) was observed at 139.8°C (The assignment was made by POM and SAXS, see below). The smectic phase of $PAChol_{16}$ was kept until to -50°C without recrystallization, while PEG block recrystallized at T_{cr} = -34.7°C. On the second heating/cooling scan, SmA_d-I and I-SmA_d of $PAChol_{16}$, as well as T_m and T_{cr} of PEG were again observed. Using POM on cooling slowly (-1°C/min) from isotropic phase, the I-LC phase transition with birefringence appearance was observed at 138.0°C with the development of the typical fan-shape textures of smectic phase. Figure 3a shows textures at 128°C and no significant change of the type of textures was observed until 25°C (see Figure S7 in SI). The fiber sample of PEG_{45}-TPE-*b*-$PAChol_{16}$ drawn at 135°C and cooled down to 25°C was studied by SAXS (Figure 3b). Two orders of

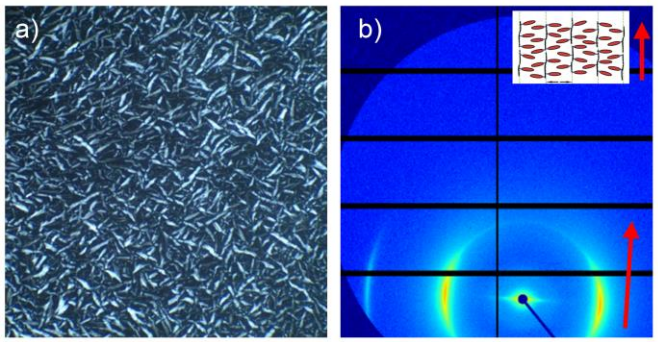

Figure 3. (a) POM image of PEG_{45}-TPE-*b*-$PAChol_{16}$ at 128°C showing typical fan-shape textures of smectic A phase. (b) SAXS pattern of PEG_{45}-TPE-*b*-$PAChol_{16}$ fiber at room temperature, which was drawn at 135°C and cooled to 25°C. The red arrow indicates the drawing direction of fiber. A layer spacing of P = 4.34 nm was measured for the smectic A phase with its layer normal perpendicular to the fiber long axis as shown in the inset of (b) (Inset: red ellipses represent mesogens and black lines polyacrylate backbones).

diffraction was detected at q_1 = 1.447 nm^{-1} and q_2 = 2.878 nm^{-1} (q_2/q_1 = 2), that are associated with a repeating distance of 4.34 nm of the smectic phase. Its 2D diffraction pattern (Figure 3b) also indicates the type A of the smectic phase with its layer normal aligned perpendicular to the fiber long axis. By comparing all these results to those of the homopolymer PAChol, we can conclude that the liquid crystal phase in the hydrophobic block of PEG_{45}-TPE-*b*-$PAChol_{16}$ is the same as that in the homopolymer, i.e., SmA_d with layer spacing d of 4.3 nm. Neither the PEG block nor the TPE moiety have disturbed the smectic phase of PAChol block. Note that in a luminescent LC polymer published recently where both TPE and Chol moieties were connected in the same side group, the presence of TPE did influence the LC phases and circularly polarized luminescence properties were achieved.[43]

The block copolymers PEG_{45}-TPE-*b*-$PAChol_n$ (n = 11, 14) showed similar phase behaviours, only transition temperatures of SmA_d-I being slightly lower ($T_{I\text{-}SmA}$ = 128.5°C for n = 11, and $T_{I\text{-}SmA}$ = 132.8°C for n = 14 on cooling at 1°C/min by POM), because of the relative high ratios of the PEG part (non-LC) in the copolymers. Their POM textures and SAXS patterns are given in SI (Figure S8-9).

3. Self-assembly of PEG_{45}-TPE-*b*-$PAChol_{16}$ by nanoprecipitation in dioxane/water and in THF/water systems

Our previous studies showed cholesterol-containing amphiphilic copolymers with PEG block ratio f_{PEG} > 15% are favourable for vesicle formation.[7,9] Therefore, PEG_{45}-TPE-*b*-$PAChol_{16}$ (f_{PEG} = 18%) has been chosen here as a representative polymer to make the self-assembly. The self-assembly of PEG_{45}-TPE-*b*-$PAChol_{16}$ was performed by nanoprecipitation using either dioxane or THF as co-solvent. The obtained self-assemblies were characterized by DLS, cryo-EM and SEM.

The cryo-EM images in Figure 4 show the morphologies of self-assemblies prepared in dioxane/water system. PEG_{45}-TPE-*b*-$PAChol_{16}$ formed elongated vesicles with ellipsoidal or tubular shapes (Figure 4a, b), which are similar to other cholesterol-based LC polymersomes. The diameter along the short axis is about 100 nm, but the size along the long axis extends to 500 nm or several microns. Some long vesicles are cut, only because of the cryo-EM sample preparation (the sample was flush frozen

in a very thin vitreous ice layer of ~ 100 nm thickness); they should have integral shapes when dispersed in water. Since DLS was not a suitable technique to characterize the non-spherical particles, SEM was used to observe the whole size of these elongated vesicles. As shown in Figure 4c, micron-sized crashed ellipsoidal or elongated objects corresponding to the dehydrated vesicles were visible. Despite the heterogeneity in the size of polymersomes, their membrane thickness was homogeneous with a value of 10 ± 1 nm as measured by statistical analysis of the cryo-EM images of 30 different vesicles. As the molecular length of one AChol unit in the extended state on the PEG_{45}-TPE-*b*-$PAChol_{16}$ copolymer chain is about 0.3 nm (calculated by Chem3D software), the maximum molecular length of the PAChol block in PEG_{45}-TPE-*b*-$PAChol_{16}$ should be 4.8 nm. This value was approximately half of the membrane thickness. It suggests that the LC polymersomes of PEG_{45}-TPE-*b*-$PAChol_{16}$ are unilamellar and the vesicle membrane has a bilayer structure in which the stretched PAChol polymers are along the normal of the membrane. Another interesting observation of the LC polymersomes obtained in dioxane/water system was that the membrane of ellipsoidal or tubular vesicles presented the periodic stripes perpendicular to their long axis (Figure 4a-c). The inset in Figure 4a shows the fast Fourier transform (FFT) giving the period of the stripe P = 4.2 nm. All these structural characteristics are similar to those observed for the polymersomes of PEG_{45}-*b*-$PAChol_{16}$ prepared in dioxane/water system.[7,9] Note that the difference between PEG_{45}-TPE-*b*-$PAChol_{16}$ and PEG_{45}-*b*-$PAChol_{16}$ is that in the former polymer an acrylate unit with a TPE side group was inserted between PEG and PAChol blocks. As shown in Figure 4d, bending of the membrane perpendicular to the layers makes the layer spacing on both sides of the membrane unequal and therefore costs extra elastic free energy. In contrast, bending the membrane parallel to the smectic layer does not change the layer spacing, and therefore is energetically favoured. Consequently, the smectic layers (stripes) are always perpendicular to the major axis of vesicles. In brief, polymersomes with smectic order in the membrane and ellipsoidal or tubular shape were also obtained from PEG_{45}-TPE-*b*-$PAChol_{16}$.

When the organic solvent in the self-assembly process was changed from dioxane to THF, spherical nanoparticles instead of elongated vesicles were obtained. Figure 5a-b show the morphologies and the size distributions of nanoparticles prepared in THF/water system in the same conditions as in dioxane/water system (the initial concentration of the copolymer in organic solvent was 2 mg/mL). Changing the initial concentration of the copolymer from 2 mg/mL to 1 mg/mL and to 10 mg/mL, respectively, the morphologies of nanoparticles kept unchanged, as shown in Figure 5c, Figure S11-12. These results are similar to those observed in PEG_{45}-*b*-$PAChol_{16}$ that also self-assembled into spherical aggregates in the THF/water system.[9]

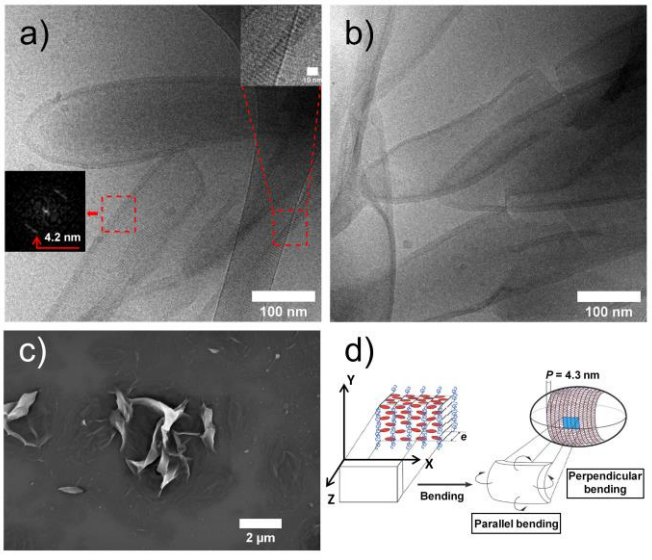

Figure 4. Cryo-EM (a-b) and SEM (c) images of the self-assemblies formed by PEG_{45}-TPE-*b*-$PAChol_{16}$ copolymer in dioxane/water system. The inset in image (a) is the fast Fourier transform (FFT) of the smectic structure present in the red rectangle. d) Schematic illustration of the aniosotropic bending of polymer bilayer with smectic stripes in an ellipsoidal polymersome (adopted from Ref. 7). Red ellipses represent mesogens, black lines polyacrylate backbones, and blue wavy lines PEG chains. Z axis is along the normal of the membrane. *e* is the membrane thickness and *P* is the smectic period.

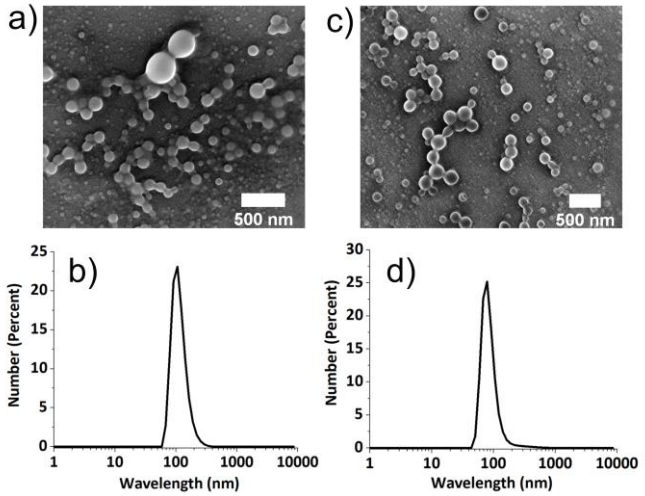

Figure 5. SEM images and size distributions by DLS (number profiles) of the self-assemblies formed by PEG_{45}-TPE-*b*-$PAChol_{16}$ in THF/water system with the initial polymer concentration of 2 mg/mL (a, b) and of 1 mg/mL (c, d), respectively.

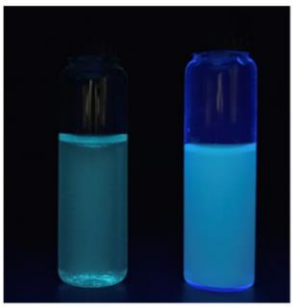

Figure 6. Photographs of PEG_{45}-TPE-*b*-$PAChol_{16}$ self-assemblies' dispersions in water observed under UV light (365 nm). Left: polymersomes obtained by nanoprecipitation in dioxane/water system. Right: spherical nanoparticles obtained by nanoprecipitation in THF/water system.

The reason why different morphologies of the self-assemblies were formed in THF/water system and dioxane/water system may reside in the different solubility of PAChol block in THF and dioxane.[9] The values of solubility parameter (δ/MPa$^{1/2}$) of solvents are δ_{THF} = 19.4 and $\delta_{dioxane}$ = 20.5.[44] Those of repeating units of polymer blocks are δ_{PEG} = 20.2 and δ_{PAChol} = 16.1, as calculated by group contribution method.[45] According to these solubility parameters, THF and dioxane are nearly equivalently good solvent for PEG. However, THF is a better solvent for PAChol than dioxane. This difference in solvent-PAChol interaction was also proved by the higher critical water concentration (CWC) for aggregation formation during the nanoprecipitation in THF/water system than in dioxane/water one.[9] We extrapolated that the PEG$_{45}$-TPE-*b*-PAChol$_n$ series should display similar behaviour, and this CWC difference was effectively demonstrated by AIE properties of PEG$_{45}$-TPE-*b*-PAChol$_{16}$ in dioxane/water and THF/water mixtures that will be discussed in the next section (see Figure 7 below). As the interaction between dioxane and PAChol is not so favourable, the interaction between PAChol and PAChol (mesogen-mesogen interaction) may be favoured upon water addition and play then an important role in the aggregate formation. We demonstrated previously that the smectic organization was a kinetic driving force for the smectic polymer aggregates in dioxane/water system.[46] Small micellar nuclei with smectic order should be formed already at the very beginning of water addition in dioxane solution. A ''liquid crystallization''-driven process leads to the growth of these nuclei and the formation of membranes with smectic stripes, that finally form elongated shapes of vesicles. In contrast, in THF/water system, THF might be expelled from both the PEG and PAChol blocks much latter upon water addition. The nature of kinetical trapping in the polymer self-assembling[47, 48] resulted in the formation of solid spherical nanoparticles with both PEG and PAChol blocks frozen inside their cores.

4. AIE properties of elongated polymersomes and spherical nanoparticles of PEG$_{45}$-TPE-*b*-PAChol$_{16}$

The AIE property of the self-assemblies formed by PEG$_{45}$-TPE-*b*-PAChol$_{16}$ copolymer were also characterized. Figure 6 shows the water dispersions of self-assemblies obtained by nanoprecipitation in dioxane/water and in THF/water systems observed under UV light (λ = 365 nm). The dispersions of polymersomes and spherical nanoparticles emit cyan fluorescence under UV light, while no fluorescence are observed in the polymer solutions in dioxane and in THF (photos not shown). In fact, PEG$_{45}$-TPE-*b*-PAChol$_{16}$ containing a TPE group between PEG and PAChol blocks is soluble in dioxane and in THF. In these solutions, the TPE is free to the intramolecular rotations that cause the non-radiative decay after UV illumination. When PEG$_{45}$-TPE-*b*-PAChol$_{16}$ is self-assembled into polymer bilayer of vesicular membrane or aggregated into spherical nanoparticles, the intramolecular rotation of TPE moieties is restricted. Consequently, under UV illumination the radiative return through fluorescence emission takes place, and the systems display a typical AIE phenomenon.

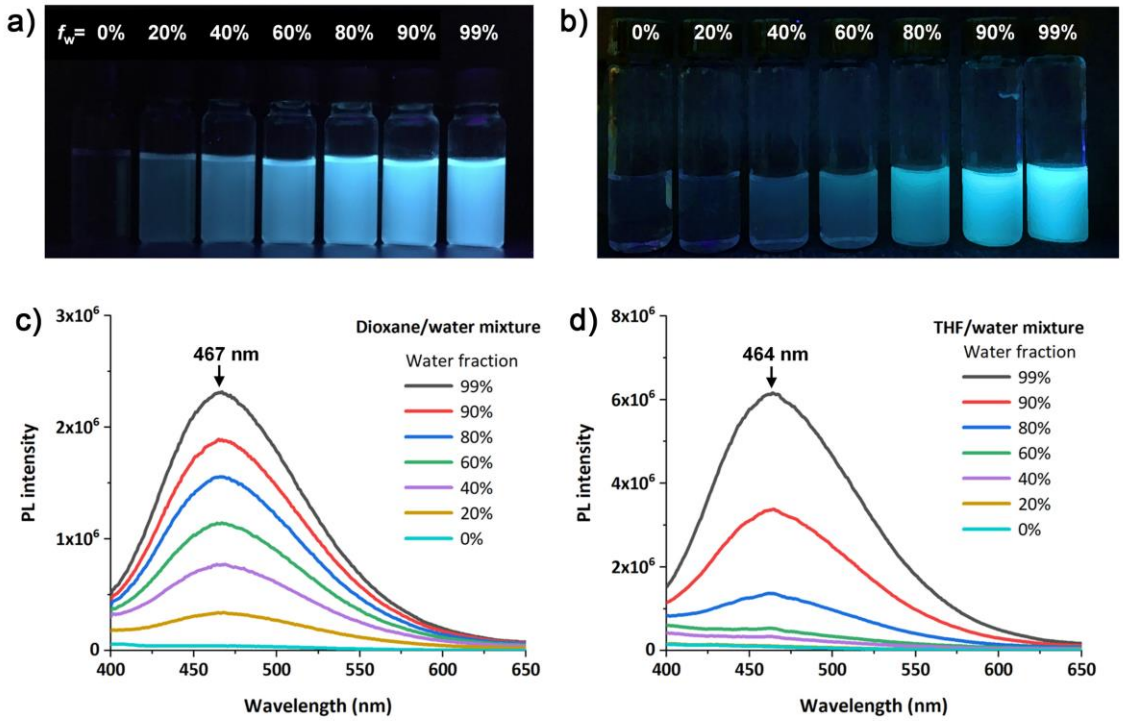

Figure 7. (a) and (c) Photographs under UV lamp (λ = 365 nm) of PEG$_{45}$-TPE-*b*-PAChol$_{16}$ in the mixtures of dioxane/water (a) and in the mixtures of THF/water (c) with the same copolymer concentration (10^{-4} mol/L) but different water fractions f_w. (b) and (d) Photoluminescence (PL) spectra of PEG$_{45}$-TPE-*b*-PAChol$_{16}$ in the mixtures of dioxane/water (b) and in the mixtures of THF/water with the same copolymer concentration (10^{-4} mol/L) but different water fractions f_w (λ_{ex}= 349 nm).

The fluorescence quantum yield of polymersomes was measured as about 0.76% by an indirect method using a standard fluorogen as reported in the literature (see SI).[42] The fluorescence quantum yield of spherical nanoparticles was measured as about 0.74%. The relative low values of quantum yield may be explained by the fact that the only one TPE group in each copolymer chain is a dangling group and located in the intersection of hydrophobic and hydrophilic domains. Consequently, the degree of restriction of TPE intramolecular rotations is relatively low. To increase the quantum yield, triblock copolymers bearing several acrylate unities with TPE side group between PEG and PAChol or after PAChol block can be designed in the future.[33-36] In addition, the AIE properties of PEG_{45}-TPE-*b*-$PAChol_{16}$ in solvent/water mixtures with different water fractions (f_w, volume) were also studied. As shown in Figure 7a, at f_w = 0%, the polymer solution in dioxane is non-emissive; at f_w = 20%, the fluorescence starts to appear. That means the aggregation occurs between 0 and 20 vol % and CWC ≤ 20 vol% in the dioxane/water system. The fluorescence becomes stronger with the increase of f_w. The characterization by fluorescence spectroscopy revealed the same phenomena as shown in Figure 7c (λ_{ex} = 349 nm). The fluorescence increase in the mixtures of THF/water (Figure 7b,d) shows the similar tendency as in the mixtures of dioxane/water, except that the AIE fluorescence appears later, *i.e.*, between 20 and 40 vol % with 20 vol% < CWC ≤ 40 vol% for aggregation. These observations are coherent with the fact that THF is a better solvent for the hydrophobic block than dioxane as above discussed.

Conclusions

A series of LC amphiphilic PEG-TPE-*b*-PAChol diblock copolymers containing a smectic LC block PAChol and an AIEgen (TPE) between hydrophilic PEG and hydrophobic PAChol blocks has been prepared by RAFT polymerization of AChol monomers using a TPE-functionalized $mPEG_{45}$ as the macro chain transfer agent (mPEG-TPE-CTA). The liquid crystal properties of the block copolymers were first characterized. The liquid crystal phase in the hydrophobic block of PEG_{45}-TPE-*b*-$PAChol_{16}$ is the same as that in the homopolymer PAChol, which is a SmA_d phase with layer spacing of 4.3 nm. Neither the PEG block nor the TPE moiety have disturbed the smectic phase of PAChol block. The copolymer PEG_{45}-TPE-*b*-$PAChol_{16}$ with a hydrophilic weight ratio of 18% was chosen for the self-assembly study using the nanoprecipitation method. The initial co-solvent (THF or dioxane) has a significant effect on the self-assembly behaviour of PEG_{45}-TPE-*b*-$PAChol_{16}$. Elongated ellipsoidal or tubular polymersomes with smectic ordering in the membrane were formed in the dioxane/water system, while spherical solid nanoparticles were obtained in THF/water system. This difference was explained by the different solubility of hydrophobic block PAChol in dioxane and in THF. All polymersomes and nanoparticles showed AIE fluorescence. Their quantum yield was around 0.7-0.8% as measured by an indirect method using a standard fluorogen. The quantum yield and brightness may be improved by introducing more AIEgen units between the hydrophilic and hydrophobic blocks. The present work shows the possibility to obtain elongated polymerosmes with both smectic LC orders and AIE fluorescence. By replacing the prototypical TPE with AIEgens that can be excited in longer wavelength than UV, these LC polymersomes and cholesterol-based nanoparticles can be designed in the future as fluorescent carriers of drugs.[13]

Author Contributions

The manuscript was written through contributions of all authors. Y.F. and M.-H.L. designed the research; N.Z., Y.F., and H.C. performed the research; H.C. and S.T. contributed to the cryo-EM imaging; A.B. contributed to the SAXS studies; N.Z., Y.F. and M.-H.L. analysed the data; M.-H.L. wrote the paper.

Conflicts of interest

There are no conflicts to declare.

Acknowledgements

This project has received financial support from the CNRS through the MITI interdisciplinary programs and the French National Research Agency (ANR-16-CE29-0028). Nian Zhang and Yujiao Fan gratefully acknowledge the China Scholarship Council for funding their PhD scholarship. The Multimodal Imaging Centre of Institut Curie is acknowledged for providing access to cryo-EM facility in Orsay.

Notes and references

1 L. Jia and M.-H. Li, *Liq. Cryst.*, 2014, **41**, 368-384.
2 X. Xing, H. Shin, M. J. Bowick, Z. Yao, L. Jia and M.-H. Li, *PNAS*, 2012, **109**, 5202-5206.
3 E. Mabrouk, D. Cuvelier, F. Brochard-Wyart, P. Nassoy and M.-H. Li, *PNAS*, 2009, **106**, 7294-7298.
4 J. Yang, D. Lévy, W. Deng, P. Keller and M.-H. Li, *Chem. Commun.*, 2005, 4345-4347.
5 J. Yang, R. Piñol, F. Gubellini, D. Lévy, P.-A. Albouy, P. Keller and M.-H. Li, *Langmuir*, 2006, **22**, 7907-7911.
6 B. Xu, R. Piñol, M. Nono-Djamen, S. Pensec, P. Keller, P.-A. Albouy, D. Lévy and M.-H. Li, *Faraday Discuss.*, 2009, **143**, 235-250.
7 L. Jia, A. Cao, D. Lévy, B. Xu, P.-A. Albouy, X. Xing, M. J. Bowick and M.-H. Li, *Soft Matter*, 2009, **5**, 3446-3451.
8 H. Yang, L. Jia, C. Zhu, A. Di-Cicco, D. Levy, P.-A. Albouy, M.-H. Li and P. Keller, *Macromolecules*, 2010, **43**, 10442-10451.
9 L. Jia, P.-A. Albouy, A. Di Cicco, A. Cao and M.-H. Li, *Polymer*, 2011, **52**, 2565-2575.
10 L. Zhou, D. Zhang, S. Hocine, A. Pilone, S. Trépout, S. Marco, C. Thomas, J. Guo and M.-H. Li, *Poly. Chem.*, 2017, **8**, 4776-4780.
11 F. Zhou, Z. Zhang, G. Jiang, J. Lu, X. Chen, Y. Li, N. Zhou and X. Zhu, *Poly. Chem.*, 2016, **7**, 2785-2789.
12 C. K. Wong, A. F. Mason, M. H. Stenzel and P. Thordarson, *Nat. Commun.*, 2017, **8**, 1240.
13 A. L. Z. Lee, S. Venkataraman, S. B. M. Sirat, S. Gao, J. L. Hedrick and Y. Y. Yang, *Biomaterials*, 2012, **33**, 1921-1928.
14 M. E. Fox, F. C. Szoka and J. M. J. Fréchet, *Acc. Chem. Res.*, 2009, **42**, 1141-1151.

15 Y. Geng, P. Dalhaimer, S. Cai, R. Tsai, M. Tewari, T. Minko and D. E. Discher, *Nat. Nanotechnol.,* 2007, **2**, 249-255.
16 D. A. Christian, S. Cai, O. B. Garbuzenko, T. Harada, A. L. Zajac, T. Minko and D. E. Discher, *Mol. Pharmaceutics*, 2009, **6**, 1343-1352.
17 L. Jia, D. Cui, J. Bignon, A. Di Cicco, J. Wdzieczak-Bakala, J. Liu and M.-H. Li, *Biomacromolecules*, 2014, **15**, 2206-2217.
18 P. P. Ghoroghchian, P. R. Frail, K. Susumu, D. Blessington, A. K. Brannan, F. S. Bates, B. Chance, D. A. Hammer and M. J. Therien, *PNAS*, 2005, **102**, 2922-2927.
19 N. A. Christian, F. Benencia, M. C. Milone, G. Li, P. R. Frail, M. J. Therien, G. Coukos and D. A. Hammer, *Mol. Imaging Biol.*, 2009, **11**, 167-177.
20 C. Murdoch, K. J. Reeves, V. Hearnden, H. Colley, M. Massignani, I. Canton, J. Madsen, A. Blanazs, S. P. Armes, A. L. Lewis, S. MacNeil, N. J. Brown, M. H. Thornhill and G. Battaglia, *Nanomedicine*, 2010, **5**, 1025-1036.
21 J. Luo, Z. Xie, J. W. Y. Lam, L. Cheng, H. Chen, C. Qiu, H. S. Kwok, X. Zhan, Y. Liu, D. Zhu and B. Z. Tang, *Chem. Commun.*, 2001, 1740-1741.
22 Y. Hong, J. W. Y. Lam and B. Z. Tang, *Chem. Commun.*, 2009, 4332-4353.
23 Y. Hong, J. W. Y. Lam and B. Z. Tang, *Chem. Soc. Rev.*, 2011, **40**, 5361-5388.
24 R. Hu, N. L. C. Leung and B. Z. Tang, *Chem. Soc. Rev.*, 2014, **43**, 4494-4562.
25 D. Ding, K. Li, B. Liu and B. Z. Tang, *Acc. Chem. Res.*, 2013, **46**, 2441-2453.
26 J. Mei, Y. Hong, J. W. Y. Lam, A. Qin, Y. Tang and B. Z. Tang, *Adv. Mater.*, 2014, **26**, 5429-5479.
27 K. Li and B. Liu, *Chem. Soc. Rev.*, 2014, **43**, 6570-6597.
28 A. Qin, Y. Zhang, N. Han, J. Mei, J. Sun, W. Fan, and B. Z. Tang, *Sci. China Chem*., 2012, **55**, 772-778.
29 H. Chen and M.-H. Li, *Chin. J. Polym. Sci*., 2019, **37**, 352-371.
30 X. Ji, Y. Li, H. Wang, R. Zhao, G. Tang and F. Huang, *Poly. Chem.*, 2015, **6**, 5021-5025.
31 M. Huo, Q. Ye, H. Che, X. Wang, Y. Wei and J. Yuan, *Macromolecules*, 2017, **50**, 1126-1133.
32 Y. Li, X. Wu, B. Yang, X. Zhang, H. Li, A. Umar, N. F. d. Rooij, G. Zhou and Y. Wang, *ACS Appl. Mater. Interfaces*, 2019, **11**, 37077-37083.
33 N. Zhang, H. Chen, Y. Fan, L. Zhou, S. Trépout, J. Guo and M.-H. Li, *ACS Nano*, 2018, **12**, 4025-4035.
34 D. Zhang, Y. Fan, H. Chen, S. Trepout and M. H. Li, *Angew. Chem. Int. Ed*., 2019, **58**, 10260-10265.
35 X. Tao, H. Chen, S. Trépout, J. Cen, J. Ling and M.-H. Li, *Chem. Commun.*, 2019, **55**, 13530-13533.
36 H. Chen, Y. Fan, N. Zhang, S. Trépout, B. Ptissam, A. Brûlet, B. Z. Tang and M.-H. Li, *Chem. Sci.*, 2021, **12**, 5495-5504
37 N. U. Deshpande, M. Virmani and M. Jayakannan, *Poly. Chem.*, 2021, **12**, 1549-1561.
38 S. Cao, J. Shao, H. Wu, S. Song, M. T. De Martino, I. A. B. Pijpers, H. Friedrich, L. K. E. A. Abdelmohsen, D. S. Williams and J. C. M. van Hest, *Nat. Commun*., 2021, **12**, 2077.
39 S. Cao, Y. Xia, J. Shao, B. Guo, Y. Dong, I. A. B. Pijpers, Z. Zhong, F. Meng, L. K. E. A. Abdelmohsen, D. S. Williams and J. C. M. van Hest, *Angew. Chem. Int.*, 2021, **60**, 17629-17637.
40 H. Zhou, J. Li, M. H. Chua, H. Yan, B. Z. Tang and J. Xu, *Poly. Chem.*, 2014, **5**, 5628-5637.
41 B. H. P. van de Kruijs, M. H. C. L. Dressen, J. Meuldijk, J. A. J. M. Vekemans and L. A. Hulshof, Org. Biomol. Chem., 2010, 8, 1688-1694.
42 H. Lu, F. Su, Q. Mei, Y. Tian, W. Tian, R. H. Johnson and D. R. Meldrum, *J. Mater. Chem*., 2012, **22**, 9890-9900.
43 Z. W. Luo, L. Tao, C. L. Zhong, Z. X. Li, K. Lan, Y. Feng, P. Wang and H. L. Xie, *Macromolecules*, 2020, **53**, 9758-9768.
44 J. E. Mark, *Physical Properties of Polymer Handbook,* 2007.
45 E. H. I. J. Brandrup, and E. A. Grulke, *Polymer handbook*, 1999.
46 L. Jia, D. Lévy, D. Durand, M. Impéror-Clerc, A. Cao and M.-H. Li, *Soft Matter*, 2011, **7**, 7395-7403.
47 S. Jain and F. S. Bates, Macromolecules, 2004, 37, 1511-1523.
48 H. Cui, Z. Chen, S. Zhong, L. Wooley Karen and J. Pochan Darrin, *Science*, 2007, **317**, 647-650.

